Characteristics of Internal Gravity Waves and Earthquake Prediction

Academician V. V. Adushkin[a], V. I. Nifadiev[b], B. B. Chen[b], S. I. Popel[c,*], G. A. Kogai[b], A. Yu. Dubinskii[c], and P. G. Weidler[d]

Abstract—On the basis of the data on perturbations in the Earth's atmosphere recorded before and after 52 significant earthquakes that occurred during the period from 1997 to 2018 in the Asian region, it is shown that the amplitudes of internal gravity waves that originated from seismically active regions can be used at the saturation threshold level for a short-term indication of upcoming seismic events.

Keywords: earthquakes, seismically active regions, internal gravity waves, amplitude of temperature perturbations, short-term earthquake forecast

The existing methods for predicting especially dangerous natural geophysical phenomena have low efficiency due to the short forecast time, which is insufficient to take appropriate measures to prevent catastrophic consequences, especially earthquakes. A short-term earthquake forecast based on physical precursors [1] is usually implemented as registration of abnormal behavior of various geophysical parameters. The question of which of those are actual precursors and which are better and more reliable, however, remains open to this day [2].

Internal gravitational waves (IGWs), generated in seismically active regions, mainly due to the release of lithospheric gases into the atmosphere (see, e.g., [3, 4]), can be regarded as one of the mechanisms of the interaction between the lithosphere and the atmosphere. These waves are recorded before and after earthquakes (see, e.g., [5, 6]). Analysis of the data on disturbances in the Earth's atmosphere before and after earthquakes in Uzbekistan on May 26, 2013, in Kyrgyzstan on January 8, 2007, and in Kazakhstan on January 28, 2013, revealed previously unknown changes in the parameters of internal gravitational waves over several days before the earthquakes [7], which in some cases can be used as a short-term forecast of an upcoming seismic event. For a better interpretation, the amount of measured data on disturbances in the Earth's atmosphere before and after earthquakes should be increased. In this paper, we analyze the IGWs observed before and after each of the 52 earthquakes with magnitudes M ≥ 5.0 (Richter scale), which occurred during the period from 1997 to 2018, to establish the possibility of using such waves as earthquake precursors. In contrast to [7], where only three earthquakes and, mainly, the behavior of the characteristic wavelengths of the IGWs were considered, here, the possibility of using the amplitudes of the IGW, from seismically active regions, for a short-term forecast of upcoming seismic events is discussed.

The convective instability in the lower and middle atmosphere resulting from the processes occurring in the lithosphere acts as the main source of IGW generation in seismically active regions (see, e.g., [8–11]). Wave energy dissipates with the IGW amplitude being at the saturation threshold [12]. The amplitudes of the IGWs found in the stratosphere and identified as precursors of earthquakes increase up to the stratopause height, then the wave dissipates [7]. Consequently, the values of real IGW amplitudes at the saturation threshold level can be used to estimate the time of upcoming seismic events.

The real IGW amplitudes at the saturation threshold level were analyzed for 52 earthquakes with magnitudes M ≥ 5.0 occurred in 1997–2018 in the Asian region. Data from [13] were used for the information about the earthquakes. In all cases, satellite data on the average atmosphere temperature recorded at 06:00 UTC above points located in random order and

[a] *Institute of Geosphere Dynamics, Russian Academy of Sciences, Moscow, 119334 Russia*
[b] *Kyrgyz Russian Slavic University, 720000 Bishkek, Kyrgyzstan*
[c] *Space Research Institute, Russian Academy of Sciences, Moscow, 117997 Russia*
[d] *Karlsruhe Institute of Technology, Campus North, Eggenstein-Leopoldshafen, D-76344 Germany*
**e-mail: popel@iki.rssi.ru*

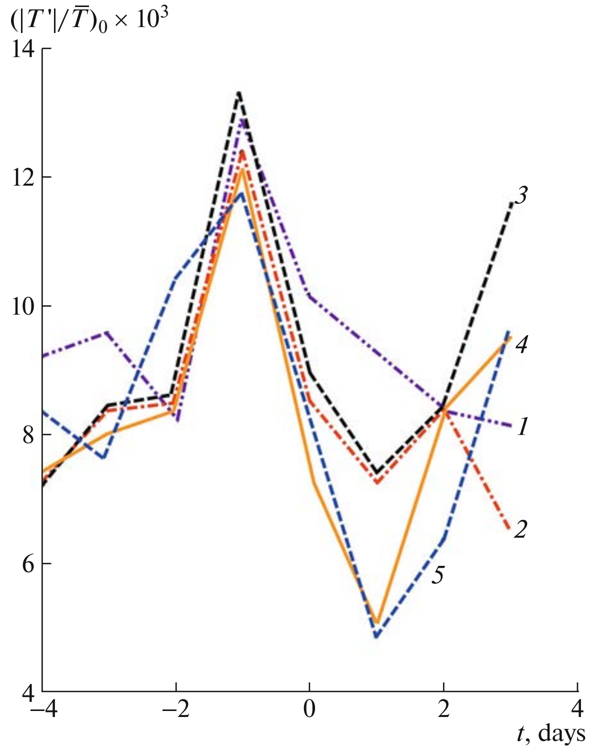

Fig. 1. Distributions of the maximum values of normalized amplitudes before and after the earthquake in Sichuan, China on May 12, 2008.

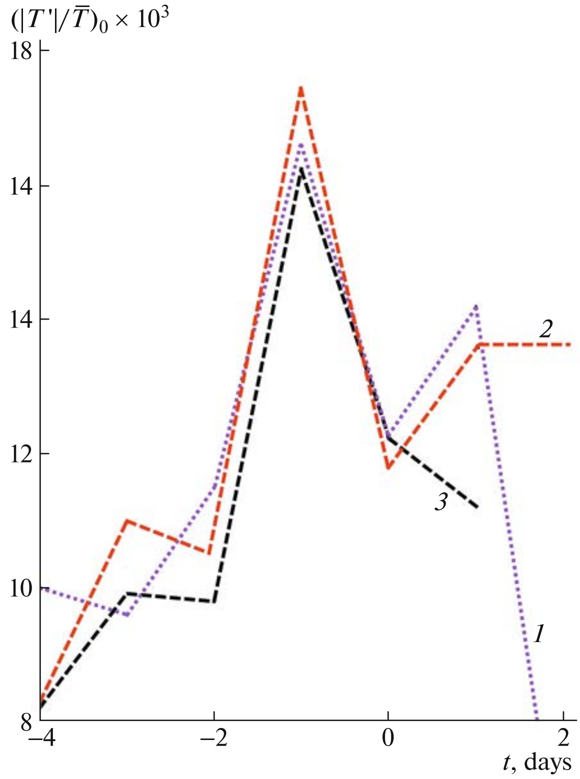

Fig. 2. Distributions of the maximum values of normalized amplitudes before and after the earthquake in Afghanistan on January 31, 2018.

at different distances from the source (epicenter) of the earthquake, available in the GIOVANNY system [14], were processed. The maximum values $(|T'|/\bar{T})_0$ of the normalized amplitudes of temperature perturbations $|T'|/\bar{T} = |T - \bar{T}|/\bar{T}$ were calculated, where T is the initial temperature profile and $\bar{T}$ is the spline profile superimposed on the temperature profile four days before the earthquake and 2–3 days after it.

The distributions of the maximum values of normalized amplitudes $(|T'|/\bar{T})_0$ four days before and three days after the well-known seismic event in Sichuan, China (depth of the hypocenter H = 19 km, Richter magnitude M = 7.9, occurred on May 12, 2008, at 06:28:01 UTC) are shown in Fig. 1. The data are given for five points located along the line between the epicenter of the earthquake and Teploklyuchenka (SE of Lake Issyk-Kul, Central Tien Shan). The curves correspond to the $(|T'|/\bar{T})_0$ distribution above the following sites: (1) Teploklyuchenka (78.5° E, 42.5° N); (2) Shayar, Aksu, XUAR, China (83.46° E, 40.2° N); (3) Ruoqiang, XUAR, China (88.42° E, 37.9° N); (4) Golmud, Qinghai, China (93.38° E, 36.6° N); (5) Sershu, Garze, Sichuan, China (98.34° E, 33.3° N). The epicenter was located in Zoige, Ngawa, Sichuan, China (103.322° E, 31.002° N).

The distribution of $(|T'|/\bar{T})_0$ before and after the earthquake in Afghanistan (depth of the hypocenter H = 193.7 km, magnitude M = 6.2 according to Richter, occurred on January 31, 2018, at 07:07:00 UTC) over the points with coordinates 72.73° E, 40.25° N (curve *1*), 74.65° E, 41.00° N (curve *2*), 76.57° E, 41.75° N (curve 3) is shown in Fig. 2.

Note that all curves in Figs. 1 and 2 display the same pattern: the magnitude of $(|T'|/\bar{T})_0$ sharply increases one day before the earthquake, then falls at the time of the earthquake, regardless of the location of the measurement point. Besides, all the plots characterizing the situation before and after nine earthquakes (Fig. 3) that occurred between 1997 and 2017, i.e., in Tajikistan on November 17, 2004 (curve *1*); Northeast Iran on April 5, 2017 (curve *2*); East Iran on May 10, 1997 (curve *3*); East Iran on February 24, 2009 (curve *4*); XUAR, China on May 11, 2017 (curve *5*); Kegen, Kazakhstan on January 28, 2013 (curve *6*); Bulungur, Uzbekistan on May 26, 2013 (curve *7*); Kadamjay, Kyrgyzstan on July 19, 2011 (curve *8*); and Kyrgyzstan on May 12, 2008 (curve *9*), clearly reveal the same pattern. This pattern, however, was only observed in cases when the earthquake hypocenters were located within several tens of kilometers from the surface. In other cases, when the hypocenters were at depths of several hundred kilometers, the probability of the revealed pattern was significantly lower.

Let us consider the behavior of the normalized wave amplitude $(|T'|/\bar{T})_0$ before, during, and after the earthquakes, using wavelet analysis as the preferable method for identifying and analyzing the structure of wave spectra. As an example, which is typical of the 52 earthquakes considered, we present a comparison of the two earthquakes in China and Afghanistan. These two earthquakes had significantly different hypocenter depths, and their magnitudes also differed. The hypocenter of the earthquake in Afghanistan (the Hindu Kush mountain range) was located at a depth of 193.7 km, and the magnitude was M = 6.2 on the Richter scale. The earthquake in Sichuan, China occurred at a much shallower depth (19.0 km) and had a magnitude of M = 7.9 on the Richter scale. Apparently, the dynamics of the release of lithospheric gases during the preparation stage of earthquakes, when the natural gases discharged create excessive concentrations of individual gases in the troposphere [15], differed, which affected the variations in the IGW normalized amplitudes. Thus, two days and one day before the Sichuan earthquake, maximums of the normalized waves were observed within 20 km above sea level. In the case of the Hindu Kush event, the maximum of the normalized amplitude was recorded two days before the earthquake. In this case, the variation maxima of the normalized amplitude were observed between the altitudes of 40 and 50 km and, apparently, were associated with the dynamics of the release of lithospheric gases from much greater depths (as compared with the situation in Sichuan). The process of the IGW dissipation before an earthquake in the Hindu Kush mountain range is more inertial than in the Sichuan earthquake. Therefore, the wave saturation occurs much later, which can be explained by differences in the geological structure of these seismically active regions and by a significant difference in the hypocenter depths of these earthquakes.

Thus, it was discovered that variations of the maximum value of the normalized amplitude of temperature perturbations of the IGWs that originated from seismically active regions follow a pattern in which the day before the earthquake, the value increases sharply and subsequently falls at the time of the earthquake, provided that the earthquake hypocenters are located at a depth of several tens of kilometers below the surface. In cases when the hypocenter is located deeper (up to several hundred kilometers), the probability of such a pattern is significantly reduced. An IGW parameter that is more indicative for forecasting earthquakes is the distribution of the normalized wave amplitude with height. The saturation of the IGW manifested in the maximum wave amplitude occurs one day before earthquakes with hypocenters at depths of several tens of kilometers from the surface. In the case of deeper hypocenter locations, IGW saturation is reached two days before the earthquake, and the process of wave energy dissipation starts later, which can be explained by differences in the geological structure of seismically active regions and a significant difference in the depths of the earthquake hypocenters. Consequently, the amplitudes of the IGWs that originated from seismically active regions at the level of the saturation threshold can be used for a short-term forecast of upcoming seismic events.

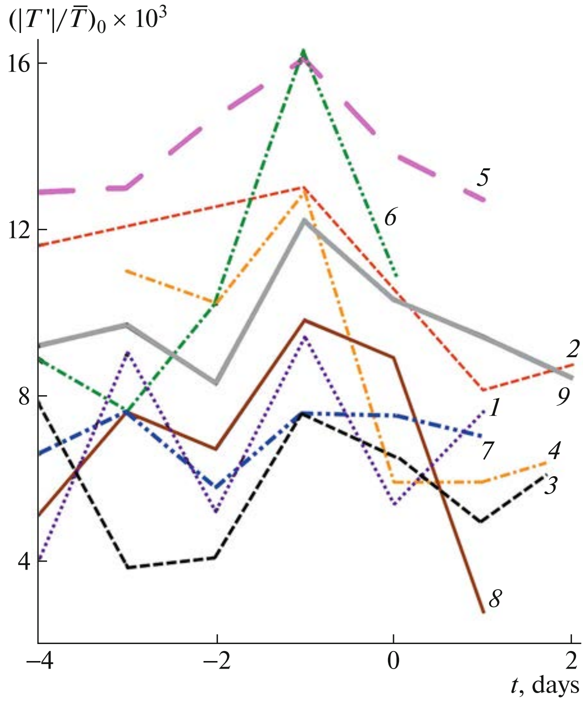

Fig. 3. Distributions of the maximum values of normalized amplitudes before and after nine major earthquakes that occurred in the Asian region from 1997 to 2017.

REFERENCES

1. C. H. Scholz, L. R. Sykes, and Y. P. Aggarwal, Science, No. 4102, 803–810 (1973).
2. R. D. Cicerone, J. E. Ebel, and J. Britton, Tectonophysics **476** (3), 371–396 (2009).
3. M. B. Gokhberg and S. L. Shalimov, Ross. Zh. Nauk Zemle **2** (2), 95–108 (2000).
4. S. L. Shalimov, *Atmospheric Waves in Ionospheric Plasma (with Geophysical Examples)* (Schmidt Institute of Physics of the Earth RAS, Moscow, 2018) [in Russian].
5. E. M. Lin'kov, L. N. Petrova, and K. S. Osipov, Dokl. Akad. Nauk SSSR **313** (5), 1095–1098 (1990).
6. K. V. Popov, V. A. Liperovsky, C.-V. Meister, P. I. Biagi, E. V. Liperovskaya, and A. S. Silina, Phys. Chem. Earth **29**, 529–535 (2004).
7. V. V. Adushkin, V. I. Nifadiev, B. B. Chen, S. I. Popel, G. A. Kogai, A. Yu. Dubinskii, and P. G. Weidler, Dokl. Earth Sci. **487** (1), 841–845 (2019).

8. D. C. Fritts, Rev. Geophys. Space Phys. **22**, 275–308 (1984).
9. D. C. Fritts and P. K. Rastogi, Radio Sci. **20** (6), 1247–1277 (1985).
10. D. C. Fritts, Pure Appl. Geophys. **130**, 343–371 (1989).
11. D. C. Fritts and M. J. Alexander, Rev. Geophys. **41** (1), 1003 (2003).
12. V. R. Gubenko and I. A. Kirillovich, Soln.-Zemn. Fiz. **4** (2), 76–85 (2018).
13. http://www.usgs.gov/natural-hazards/earthquake-hazards/earthquakes.
14. https://giovanny.gsfc.nasa.gov/giovanny/#service=Vt&=MA13CPASMv5_2_0.
15. G. I. Voitov and I. P. Dobrovol'skii, Fiz. Zemli, No. 3, 20–31 (1994).

Translated by M. Hannibal